This article is published in *The Plant Cell* Online, *The Plant Cell* Preview Section, which publishes manuscripts accepted for publication after they have been edited and the authors have corrected proofs, but before the final, complete issue is published online. Early posting of articles reduces normal time to publication by several weeks.

The *Decreased apical dominance1/Petunia hybrida CAROTENOID CLEAVAGE DIOXYGENASE8* Gene Affects Branch Production and Plays a Role in Leaf Senescence, Root Growth, and Flower Development

Kimberley C. Snowden,[a] Andrew J. Simkin,[b] Bart J. Janssen,[a] Kerry R. Templeton,[a] Holly M. Loucas,[c] Joanne L. Simons,[a] Sakuntala Karunairetnam,[a] Andrew P. Gleave,[a] David G. Clark,[c] and Harry J. Klee[b,1]

[a] HortResearch, Private Bag 92169, Mt. Albert, Auckland, New Zealand
[b] Plant Molecular and Cellular Biology Program, University of Florida, Gainesville, Florida 32611-0690
[c] Environmental Horticulture, University of Florida, Gainesville, Florida 32611-0670

Carotenoids and carotenoid cleavage products play an important and integral role in plant development. The *Decreased apical dominance1* (*Dad1*)/*PhCCD8* gene of petunia (*Petunia hybrida*) encodes a hypothetical carotenoid cleavage dioxygenase (CCD) and ortholog of the *MORE AXILLARY GROWTH4* (*MAX4*)/*AtCCD8* gene. The *dad1-1* mutant allele was inactivated by insertion of an unusual transposon (*Dad-one transposon*), and the *dad1-3* allele is a revertant allele of *dad1-1*. Consistent with its role in producing a graft-transmissible compound that can alter branching, the *Dad1*/*PhCCD8* gene is expressed in root and shoot tissue. This expression is upregulated in the stems of the *dad1-1*, *dad2*, and *dad3* increased branching mutants, indicating feedback regulation of the gene in this tissue. However, this feedback regulation does not affect the root expression of *Dad1*/*PhCCD8*. Overexpression of *Dad1*/*PhCCD8* in the *dad1-1* mutant complemented the mutant phenotype, and RNA interference in the wild type resulted in an increased branching phenotype. Other differences in phenotype associated with the loss of *Dad1*/*PhCCD8* function included altered timing of axillary meristem development, delayed leaf senescence, smaller flowers, reduced internode length, and reduced root growth. These data indicate that the substrate(s) and/or product(s) of the *Dad1*/*PhCCD8* enzyme are mobile signal molecules with diverse roles in plant development.

INTRODUCTION

The architecture of plants is diverse and ranges from a simple unbranched shoot system (e.g., a monopodial palm tree) to the complex multiply branched shoot systems, classified into 23 distinct architectural patterns (Hallé, 1999), seen in most trees. The development of complex shoot systems and branching patterns is a dynamic process that continues throughout the life of the plant by progressive addition of new shoot modules. In flowering plants, additional shoots originate from meristematic centers that form within the leaf axils through a process called lateral branching (Steeves and Sussex, 1989). The diversity and architectural complexity found in plants are the result of several processes. Distribution of lateral shoots is an important first step in establishing the overall architecture of the plant. However, placement of branches alone is not sufficient to produce the diversity of branch patterns seen in nature. Other developmental programs play important roles in determining the final form of the plant. These include both initiation and duration of shoot growth, differential growth rates of lateral and main shoots, angle (orthotropic versus plagiotropic) of branch growth, and branch ontogeny (monopodial versus sympodial development; Steeves and Sussex, 1989; Sussex and Kerk, 2001). These developmental processes can be summarized in terms of meristem development as position, identity (or potential identity), and timing of meristem activity (Bell, 1991). It is important to note that these developmental processes do not occur in isolation but rather as a dynamic interactive network responding to genetic and environmental cues (Bell, 1991).

Mutational approaches to the study of lateral branch development have been undertaken in multiple plant species (Napoli et al., 1999). Relatively nonpleiotropic mutants include the *decreased apical dominance* (*dad*) mutants of petunia (*Petunia hybrida*; Napoli, 1996; Napoli and Ruehle, 1996; Napoli et al., 1999; Snowden and Napoli, 2003), the *ramosus* (*rms*) mutants of pea (*Pisum sativum*; Beveridge, 2000; Morris et al., 2001; Rameau et al., 2002; Beveridge et al., 2003), and the *more axillary growth* (*max*) mutants of *Arabidopsis thaliana* (Stirnberg et al., 2002; Turnbull et al., 2002; Sorefan et al., 2003). The *MAX2*, *MAX3*, *MAX4*, and *RMS1* genes have been cloned (Stirnberg et al., 2002; Sorefan et al., 2003; Booker et al., 2004), with *MAX4* (*AtCCD8*) and *RMS1* being orthologous members of a family of

[1] To whom correspondence should be addressed. E-mail hjklee@ifas.ufl.edu; fax 352-846-2063.
The authors responsible for distribution of materials integral to the findings presented in this article in accordance with the policy described in the Instructions for Authors (www.plantcell.org) are: Kimberley C. Snowden (ksnowden@hortresearch.co.nz) and Harry J. Klee (hjklee@ifas.ufl.edu).
Article, publication date, and citation information can be found at www.plantcell.org/cgi/doi/10.1105/tpc.104.027714.

carotenoid cleavage dioxygenases (CCDs) of which *MAX3* (*AtCCD7*) is also a member. The isolation of multiple types of branching mutants indicates that control of lateral branching is both plastic and multigenic.

The CCD family includes proteins from both plants and animals that are known to act upon carotenoid substrates. In animals, examples include CCDs involved in synthesis of vitamin A (von Lintig and Vogt, 2000; Redmond et al., 2001; von Lintig et al., 2001; Lindqvist and Anderson, 2002) and RPE65, which binds all-*trans*-retinyl esters and is involved in regeneration of 11-*cis*-retinol in the visual cycle (Redmond et al., 1998; Gollapalli et al., 2003; Mata et al., 2004). In bacteria, enzymes in this family have substrates other than carotenoids (e.g., lignostilbene dioxygenases [LSDs]; Kamoda and Saburi, 1993a, 1993b). In plants, the founding member of the CCD family was Vp14, a 9-*cis*-epoxycarotenoid dioxygenase (NCED). This and closely related dioxygenases catalyze the 11,12 double bond cleavage of 9-*cis*-violaxanthin and 9-*cis*-neoxanthin to produce xanthoxin (Schwartz et al., 1997; Tan et al., 1997), which is subsequently converted to the phytohormone abscisic acid (ABA). Several additional plant CCDs that cleave carotenoids into apocarotenoids at different double bonds also have been identified (Schwartz et al., 2001; Bouvier et al., 2003a, 2003b; Simkin et al., 2004a, 2004b). Of particular significance are CCD7/MAX3 and CCD8/MAX4. The former enzyme cleaves multiple carotenoids at the 9,10 double bond (Booker et al., 2004). The latter enzyme has been shown to further cleave 10′-apo-β-carotenal, the 9,10 cleavage product of β-carotene, to yield 13-apo-β-carotenone (Schwartz et al., 2004). These data are consistent with CCD7 and CCD8 acting in the same pathway to produce a novel apocarotenoid phytohormone.

In petunia, growth is monopodial before flowering, with lateral branching occurring in two different patterns (Snowden and Napoli, 2003). During vegetative growth, basal lateral branches develop acropetally from nodes in a defined zone that is preceded and followed by zones where lateral branching is inhibited. After flowering, the main axis of growth is continued with a series of sympodial branches. In addition, apical branching develops in a basipetal direction and is restricted to the distal-most nodes of the monopodial axis. When grown in short days, the main axis is retarded and basal branching extended. The *dad1-1* mutant has increased lateral branching compared with wild-type V26. There is no initial zone of branch inhibition, the branch potential (percentage of nodes with a branch) is increased, and there is no change in lateral branch development in short days (Napoli, 1996; Napoli and Ruehle, 1996; Snowden and Napoli, 2003).

Formation of lateral branches has historically been considered in terms of the repression of lateral bud outgrowth by auxin derived from the apical meristem (Napoli et al., 1999). However, analysis of the *dad* mutants in petunia (Napoli, 1996; Napoli and Ruehle, 1996) and the *rms* mutants in pea (Beveridge, 2000; Morris et al., 2001) provides strong evidence for the role of other plant organs, such as roots, generating other signal molecules that control axillary bud outgrowth. Some of the petunia (*dad1* and *dad3*) and pea (*rms1*, *rms2*, and *rms5*) mutants can be reverted to the wild type by grafting to wild-type rootstocks (Beveridge et al., 1994; Napoli, 1996; Foo et al., 2001; Morris et al., 2001; C.A. Napoli and K.C. Snowden, unpublished data), and in the case of petunia by an interstock of wild-type tissue placed between mutant roots and scion (Napoli, 1996). Similar results have been reported for the Arabidopsis *max1*, *max4*/*AtCCD8*, and *max3*/*AtCCD7* mutants (Turnbull et al., 2002; Sorefan et al., 2003; Booker et al., 2004). These results suggest that wild-type roots can inhibit lateral branch outgrowth by production of a novel unidentified inhibitor of branching that is transported through graft unions. However, the observation by Napoli (1996) that mutant *dad1-1* root development above the graft union blocks restoration of the wild-type phenotype suggests an alternative model; roots produce an inducer of lateral shoot growth that is degraded by the *Dad1* gene product. In either case, identification of the novel modulator(s) of lateral branch outgrowth remains a tantalizing goal.

Similar branching phenotypes between the *dad1-1* mutant and the *max4* and *rms1* mutants and, in particular, the ability to revert the mutant phenotype to the wild type by grafting of mutant scions onto wild-type rootstocks suggested that a homolog of the *MAX4*/*RMS1* genes might be mutated in *dad1-1*. In this article, we report the cloning and characterization of the gene responsible for the *dad1* mutation in petunia. Sequencing of three mutant alleles of *dad1*, complementation of the *dad1-1* mutant in transgenic plants, as well as the phenotypes of RNA interference (RNAi) transgenic plants all confirmed that the *Dad1* gene is a member of the CCD gene family with a role in branch development.

RESULTS

Phenotypes of *dad1* Alleles

The *dad1-1* mutant was isolated and described by Napoli and Ruehle (1996) and further characterized with respect to its branching phenotype (Napoli, 1996; Snowden and Napoli, 2003). This mutant has a highly branched growth habit that can be reversed by micrografting (Napoli, 1996). We have isolated two additional alleles of *dad1* (Figure 1A) and characterized their growth in comparison with the *dad1-1* allele. The *dad1-2* allele was discovered in the background of the *dad2* branching mutant. A third *dad1* allele (*dad1-3*) was generated by ethyl methanesulfonate (EMS) mutagenesis of *dad1-1*, performed to look for second-site suppressors. During screening of this population, a line that had reverted to a near wild-type phenotype was isolated. Allelism tests showed that this line was a new allele of *dad1*, with a phenotype very similar to the wild type (a potential revertant of *dad1-1*).

Quantitative comparisons between wild-type V26 and the *dad1* alleles are shown in Figure 1B. A diagram of the patterns of lateral branching in V26 and the *dad1* mutant alleles is shown in Figure 1C. Under the growth conditions used for these experiments, V26 plants produced four branches from nodes 2 to 7 (where the cotyledonary node is counted as node 0, i.e., V26 branches from the second node above the cotyledons) with no branching from the cotyledonary node. As described previously by Napoli (1996), the *dad1-1* allele produced branches from every node up to node 10, including both axils at the cotyledonary node. For each of the branching traits measured,

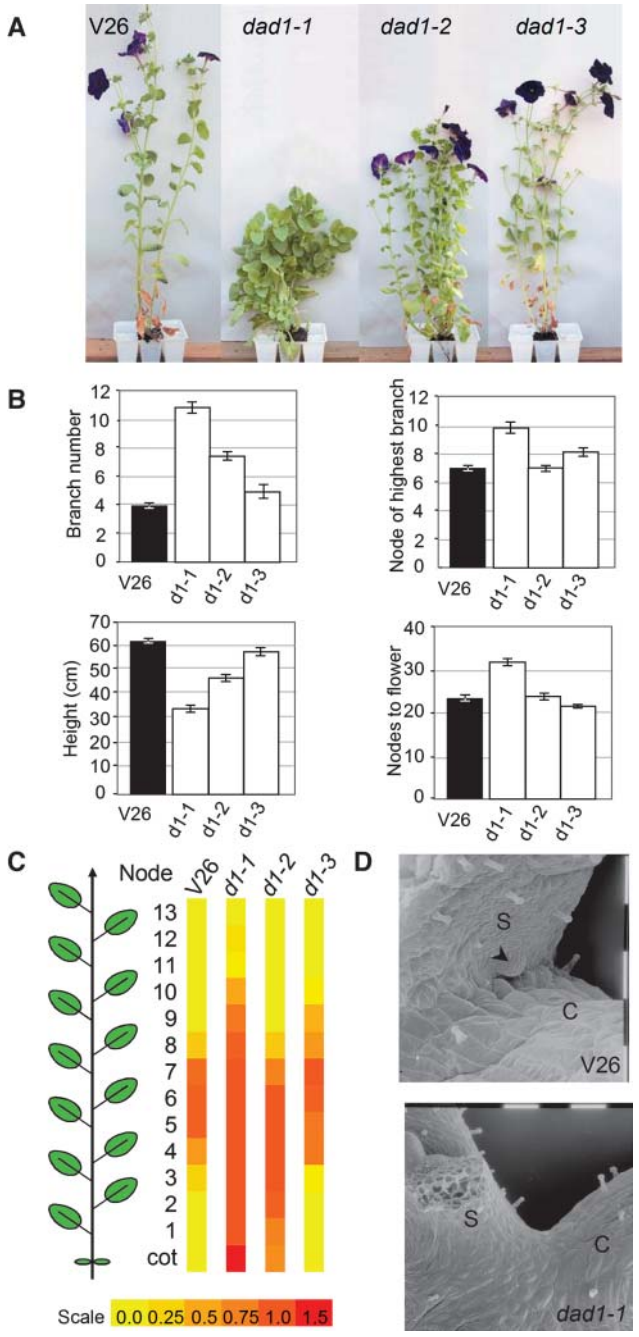

Figure 1. Phenotype of *dad1* Alleles.

(A) Wild-type V26, *dad1-1*, *dad1-2*, and *dad1-3* plants after 12 weeks of growth.

(B) Quantitative phenotypic analysis of V26 and *dad1* mutant alleles. Plants were grown for 12 weeks as described in Methods. Number of branches, overall height, the node of the highest branch, and the number of nodes to the first flower were measured for the wild type, *dad1-1* (*d1-1*), *dad1-2* (*d1-2*), and *dad1-3* (*d1-3*; $n = 16$ for each genotype). Mean values ± SE are shown.

(C) Branch distribution within wild-type and *dad1* alleles. The colored bars represent the proportion of plants ($n = 16$ for each genotype) that had a branch at that node. The value for the cotyledonary node (cot) is >1.0 when there is a branch at >1 cotyledonary axil (1 node) for the majority of the plants.

(D) Scanning electron micrographs of V26 and *dad1-1* plants. Seedlings were germinated in vitro and grown until the first true leaves were ~2 mm in length. The cotyledonary axils are shown. The gray scale bars in each photograph are 0.1 mm in length. S, main shoot; C, cotyledon. Arrowhead on the wild type (V26) indicates axillary meristem.

dad1-1 had the most extreme phenotype with more branches, more nodes that produced branches, and a greater percentage of nodes with branches.

Although it is possible to distinguish *dad1-3* branching from V26 in some growth conditions, there was no significant difference in branching pattern between *dad1-3* and V26 in the controlled growth experiments shown in Figures 1A and 1B.

The *dad1-2* allele displayed a branching phenotype intermediate between *dad1-1* and V26. As found for V26, *dad1-2* did not produce branches from nodes higher than node 7. However, branches were observed at the cotyledonary node in many (10 out of 16) of the *dad1-2* plants (Figure 1C). In addition, the *dad1-2* allele had a greater percentage of nodes with a branch than V26, the combination of both factors resulting in more branches in the *dad1-2* mutant allele than in V26.

All three *dad1* alleles reduced the overall height of the plant, although in some experiments the difference between V26 and *dad1-3* was not significant. The flowering time, as measured by the number of nodes to first flower, was increased for *dad1-1* compared with V26. The *dad1-2* allele showed no significant delay in flowering, and the *dad1-3* showed a slight but statistically significant reduction in flowering time.

While comparing the growth habit of the *dad1* alleles, we noticed that leaf senescence appeared to be altered for the *dad1-1* and *dad1-2* alleles, with older (lower node) leaves having delayed senescence (Figure 1A). In V26 plants, leaves at lower nodes went through a rapid browning and collapse of leaf structure; this leaf senescence was delayed in *dad1-1* and *dad1-2* mutants and was distinct from the slight chlorosis reported previously by Napoli (1996) for all *dad1-1* leaves. A comparison of the node number of the oldest green leaf showed a significant difference between V26, in which the oldest green leaf was at node 15.6 ± 0.3, compared with *dad1-1* at node 8.6 ± 0.5 and *dad1-2* at node 12.7 ± 0.3.

V26 and *dad1-1* Cotyledonary Branching

The early stages of branch development in *dad1-1* and V26 plants were examined using scanning electron microscopy of the cotyledonary axils of seedlings. Seedlings of both *dad1-1* mutants and V26 were examined at the same stage of development when the first true leaves had emerged and were ~2 mm in length. Altogether 25 *dad1-1* cotyledonary axils and 27 wild-type cotyledonary axils were examined (Table 1). For 21 of 27 V26 axils, a meristem-like structure was observed, and in 11 of those cases the meristem showed shoot or leaf development as well. The meristems seen in V26 axils were located on the main stem and were aligned with the midrib of the subtending cotyledon (Figure 1D). Interestingly, in 14 of 25 *dad1-1*

Table 1. Axillary Meristem Formation in Cotyledonary Nodes of *dad1-1* and V26 Seedlings

Genotype	No Meristem	Possible CAM	CAM	Leaf/Shoot formed	Total
dad1-1	14	3	6	2	25
V26	6	0	10	11	27

CAM, cotyledonary axillary meristem. Possible CAM refers to a slight swelling of cells but not a recognizable meristem.

cotyledonary axils, no meristem-like structure was observed. For seedlings for which it was possible to score all cotyledonary axils, the mean number of meristems observed for V26 was 1.54 ± 0.18 ($n = 13$) and for *dad1-1* was 0.75 ± 0.18 ($n = 12$). This result contrasts with the observation that V26 does not produce branches from the cotyledonary nodes, whereas *dad1-1* does produce branches from the cotyledonary nodes.

Isolation of *PhCCD8*

The phenotype of the petunia *dad1-1* mutant (Napoli and Ruehle, 1996) is similar to that found for the Arabidopsis *max4* (Stirnberg et al., 2002) and the pea *rms1* mutants (Rameau et al., 1997). Based on sequence comparisons of the Arabidopsis *MAX4* gene and pea *RMS1* gene (Sorefan et al., 2003), degenerate oligonucleotides were designed and used to amplify a DNA fragment from V26 petunia root and stem cDNA. A 1030-bp fragment with strong sequence similarity to the family of CCDs that includes *MAX4* and *RMS1* was amplified. A combination of PCR and inverse PCR from genomic DNA was used to obtain 5240 bp of sequence of the *PhCCD8* gene including intron sequences, 1050 bp of sequence upstream of the start codon, and 280 bp of sequence downstream of the stop codon. RT-PCR from a mixture of stem and root mRNA was used to amplify a full-length cDNA clone (1736 bp including an open reading frame [ORF] of 1668 bp), which was sequenced to confirm exon-intron boundaries (Figure 2A).

A copy of this gene also was isolated from wild-type Mitchell Diploid (MD) petunia using a similar approach with degenerate oligonucleotides to amplify a gene fragment from MD genomic DNA and using genome walker technology to obtain the full genomic sequence. Comparison of the predicted amino acid sequences from the two petunia lines showed 98% amino acid identity. The predicted PhCCD8 amino acid sequence from V26 (and MD) was 60% (61%) identical to MAX4 and 74% (74%) identical to RMS1 (MAX4 and RMS1 are 62% identical).

The *PhCCD8* gene belongs to a family of related sequences present in the animal, plant, and bacterial kingdoms. A series of iterative BLAST searches (Altschul et al., 1990) was used to identify sequences related to the *PhCCD8* gene. The *PhCCD8* gene falls into a large family of related genes, many of which have CCD activity (Figure 2E). As expected, the *PhCCD8* gene falls in a well-supported clade with the Arabidopsis gene *MAX4*/At*CCD8*, the pea gene *RMS1*, and two rice (*Oryza sativa*) genes. Using DNA gel blot analysis, *PhCCD8* was determined to be a single copy gene in petunia (data not shown); from these data we conclude that *PhCCD8* is the ortholog of *MAX4* and *RMS1*.

dad1-1 and *dad1-2* Mutants Contain Lesions in the *Dad1*/*PhCCD8* Gene

Direct sequencing of PCR products was used to determine the sequences of *dad1* mutants over the entire coding region plus upstream regions of *PhCCD8* (Figure 2A). The *dad1-1* mutant was found to contain an 1100-bp insertion in the second exon and a 10-bp direct duplication of the *Dad1*/*PhCCD8* sequence at each end of the insertion. This insertion was predicted to lead to premature termination of the Dad1/PhCCD8 protein (Figure 2B). RT-PCR was performed on mRNA from V26 and *dad1-1* root tissue using primers that would be expected to amplify overlapping fragments covering the entire ORF. RT-PCR fragments from the majority of the gene were unchanged between V26 and *dad1-1*. The sequence of an RT-PCR fragment covering the second exon revealed that the insertion did not alter RNA splicing and confirmed that the mRNA contains a premature termination codon.

A second *dad1* mutant allele (*dad1-2*) was found to contain an A-to-C transversion that results in a Tyr-to-Ser substitution in the predicted protein sequence (Figure 2A). This Tyr is conserved in many of the plant CCDs and may be involved in activity of the gene (Figure 2C).

EMS-Induced Reversion of *dad1-1* Resulted in Excision of an Unusual Transposon

Sequencing of the *Dad1* gene in the *dad1-3* line showed that the large insertion found in the *dad1-1* allele had excised, leaving a 9-bp footprint that introduced three additional amino acids (Figures 2A and 2B) relative to the wild-type sequence. This result indicates that the *dad1-3* allele, which was generated from mutagenesis of *dad1-1*, was a revertant.

Sequence analysis of the insertion found in the *dad1-1* allele revealed the presence of several repeat structures within the insertion sequence (Figure 2D). However, no terminal repeats were identified. The excision of the insertion sequence, the presence of the 9-bp footprint, and the 10-bp direct repeat of the target site all suggest that the insertion found in *dad1-1* is a transposable element (*Dot* for *Dad-one transposon*). However, the lack of terminal repeats or of any sequence similarity to known transposon sequences suggests that an unusual type of transposable element was responsible for the *dad1-1* mutation. DNA gel blot analysis using the insertion sequence as a probe revealed the presence of multiple homologous sequences within the petunia genome (data not shown).

The Insertion in the *Dad1*/*PhCCD8* Gene Cosegregates with the *dad1-1* Mutant Phenotype

Two segregating populations of *dad1-1* (in the inbred V26 background) were generated by outcrossing to other inbred lines of petunia (M1 and R54) and then selfing the F1 progeny to produce families that segregated for the *dad1-1* phenotype. Individuals were then scored by PCR using oligonucleotide primers designed to distinguish between mutant and wild-type alleles of the *Dad1*/*PhCCD8* gene. All progeny that showed the *dad1-1* phenotype in both independent populations (R54 population 24 *dad1-1* phenotype plants out of 89 total plants; M1

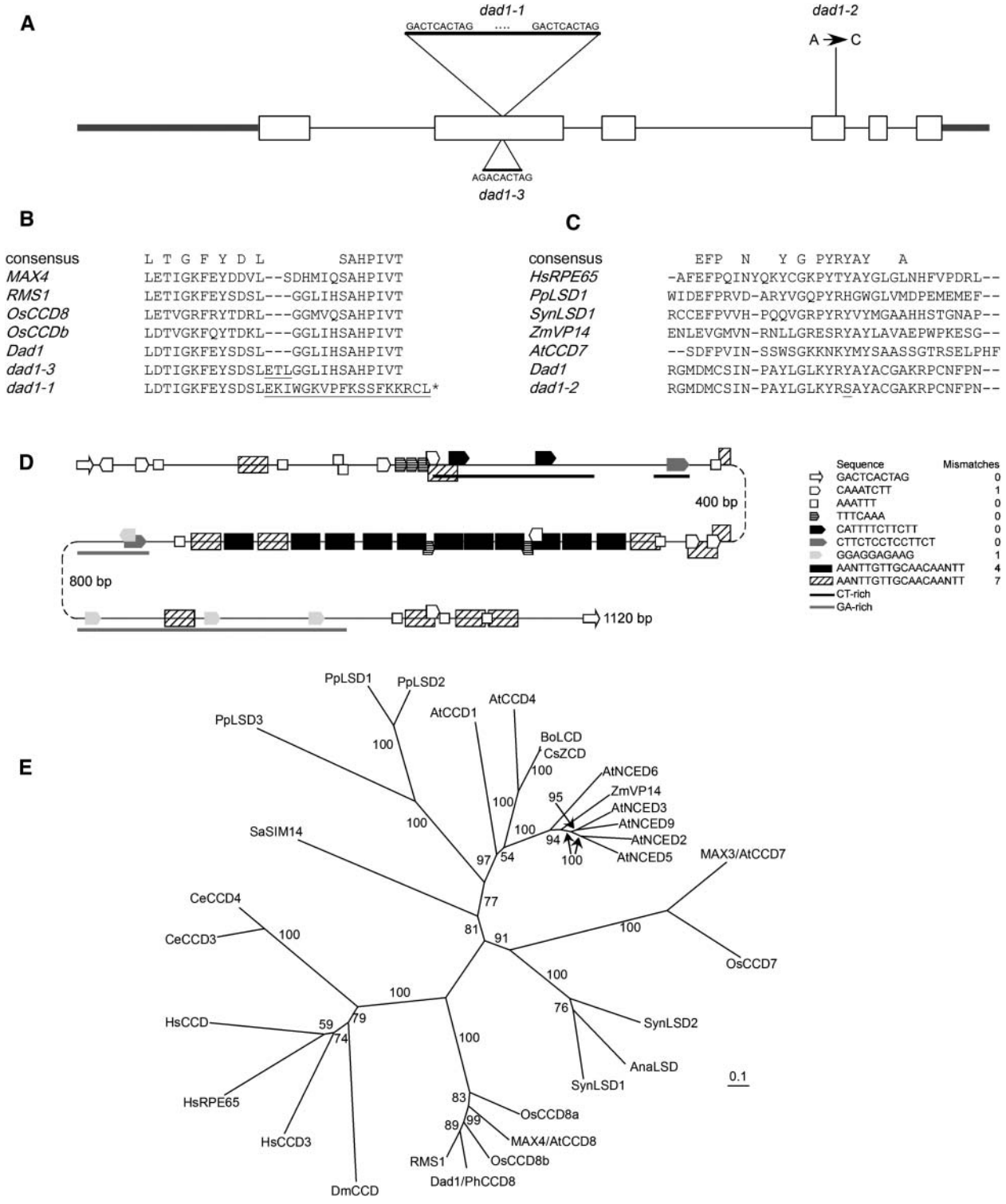

Figure 2. Structure of the *Dad1*/*PhCCD8* Gene.

(A) Structure of the *Dad1*/*PhCCD8* gene showing the locations of the mutant alleles. Open boxes represent the ORF within the exons, with introns represented by thin black lines. The promoter and 5′ and 3′ UTRs are denoted by shaded bars. The sequence associated with the *dad1-1* allele represents the *Dad1*/*PhCCD8* sequence that was duplicated by the insertion of a transposon (the actual transposon sequence is not shown), and the sequence associated with the *dad1-3* allele is the 9-bp footprint left by the excision of the transposon. For *dad1-2*, the single base change is shown.

population 30 out of 148) contained PCR products consistent with the presence of the *dad1-1* allele. These results provided genetic confirmation that the *Dad1*/*PhCCD8* gene is linked to the *dad1-1* phenotype.

Expression of *Dad1*/*PhCCD8* Complements the *dad1-1* Mutation in Transgenic Plants

To determine whether expression of *Dad1*/*PhCCD8* transgenes could complement *dad1* mutants, we used Agrobacterium-mediated transformation into *dad1-1* mutant petunia plants to introduce a cDNA copy of the V26 *Dad1* gene fused to the 35S promoter of the *Cauliflower mosaic virus* (CaMV). In 7 out of 10 plants transformed with the 35S cDNA construct, the highly branched phenotype was significantly reduced and the height of the plants was increased, resulting in plants indistinguishable from wild-type V26 (Figure 3A).

Downregulation of *Dad1*/*PhCCD8* in Wild-Type Plants Phenocopies the *dad1* Mutant

To test whether we could phenocopy the *dad1* mutation, we transformed V26 with an RNAi construct under the control of the CaMV 35S promoter. In six out of eight wild-type plants transformed with this construct, the number of branches was increased and the plant height was reduced, resulting in a phenotype very similar to the *dad1-1* mutant (Figure 3A).

Wild-type MD plants were also transformed with an RNAi construct under the control of the constitutively expressed 35S promoter of the *Figwort mosaic virus*. Gene expression in *Dad1*/*PhCCD8* RNAi lines decreased to undetectable levels in root tissue of selected lines (Figure 4A). Three independent transgenic lines showing the greatest degree of RNAi were selected for further study.

Transgenic and control lines were grown for phenotypic characterization. The RNAi lines had a highly branched phenotype visibly different from the wild type. The branching phenotype was visible 3 weeks postgermination (data not shown) and became more noticeable throughout development (Figure 3B). At 14 weeks postgermination, a significant difference between the RNAi lines and the wild type was observed (Figure 3C). This difference is more easily observed in plants stripped of their leaves (Figure 3D).

In addition to altered lateral shoot growth, several other phenotypic changes were observed. The dry weights of leaves and stems were determined for each of the three RNAi lines at 14 weeks postgermination (Table 2). A significant decrease in the dry weight of the RNAi lines compared with MD was observed. Furthermore, a significant difference in the ratio of leaf to stem matter was observed, increasing from a ratio of 1.8 to 2.7.

MD plants had an average of 21 nodes between the cotyledon and the terminal flower of the primary stem. Suppression of *Dad1*/*PhCCD8* led to a significant increase in node number before flowering, increasing to 31 to 34 nodes, similar to the result observed for *dad1-1* (Figures 1B and 5A). The flowering time for RNAi plants increased from 14 to 18 weeks (data not shown). The MD RNAi lines showed reduced flower weight (Figure 5B) and size (Figure 5C). This difference in flower size also was observed in *dad1-1* (Figures 5B and 5C).

Because *Dad1*/*PhCCD8* transcripts are primarily found in the root tissue, we examined how *Dad1*/*PhCCD8* interference affected root development. *Dad1*/*PhCCD8* RNAi led to a reduction in root mass 12 weeks postgermination (Figure 6A). A reduction in root mass in the *dad1-1* mutant compared with V26 was also observed (Table 3). However, no obvious changes in root structure were observed (Figure 6B).

Figure 2. (continued).

(B) Alignment of the predicted amino acid sequence of the *Dad1* wild-type and mutant alleles around the position of the insertion in *dad1-1*, in comparison with other members of the CCD8 clade. The consensus sequence shows amino acids that are absolutely conserved in the sequences shown (the mutant alleles were not used in consensus generation). The differences between the wild-type *Dad1* sequence and the mutant alleles are underlined. In *dad1-1*, the asterisk indicates a stop codon.

(C) Alignment of the *Dad1* and *dad1-2* predicted amino acid sequence in comparison with one member of each clade of the CCD gene family. The consensus shows amino acids for which at least three members have the sequence shown (the *dad1-2* sequence was not used in the consensus generation). The changed amino acid in the *dad1-2* allele is underlined.

(D) Repeat structure of the transposon (*Dot*) inserted in the *dad1-1* allele, including the 10-bp direct duplication of the *Dad1* sequence. The key shows the consensus sequence for each motif found in the transposon sequence with the maximum number of mismatches allowed for inclusion in the figure. The longer CT-rich region is composed of 93% CT and the shorter region is 100% CT, whereas the GA-rich region is 89% GA.

(E) Unrooted phylogenetic tree of the CCD gene family. Only full-length members of the family are included, and not all members in the NCED clade are included for clarity (though all known Arabidopsis members of the gene family are included). The predicted protein sequences were initially clustered using ClustalX (Thompson et al., 1997) and the alignment refined manually with the program MacClade (Maddison and Maddison, 2000). Phylogenetic relationships between the family members were determined using the neighbor-joining method and bootstrap analysis with 1000 replicates using the Phylip package of programs (Felsenstein, 2004). Bootstrap values are shown as percentages. Accession numbers for sequences used from the following species are as follows: Arabidopsis AtCCD1 (At3g63520), AtNCED2 (At4g18350), AtNCED3 (At3g14440), AtCCD4 (At4g19170), AtNCED5 (At1g30100), AtNCED6 (At3g24220), AtCCD7 (At2g44990), AtCCD8 (At4g32810), and AtNCED9 (At1g78390); *Bixa orellana* BoLCD (AJ489277.1); *Crocus sativus* CsZCD (CAD33262.1); *Zea mays* ZmVP14 (U95953.1); rice OsCCD7 (AL663000.4), OsCCD8a (AP003296.3), and OsCCD8b (AP003376.3); petunia Dad1/PhCCD8 (AY743219); pea RMS1 (AY557341.1); *Sphingomonas paucimobilis* PpLSD1 (S80637.1), PpLSD2 (S65040.1), and PpLSD3 (AB073227.1); *Streptomyces antibioticus* SaSIM14 (AF322256.1); *Synechocystis* sp SynLSD1 (D90914.1) and SynLSD2 (AP005369.1); *Anabaena* sp AnaLSD (AP003595.1); *Homo sapiens* HsRPE65 (AF039855.1), HsCCD (AJ290393.1), and HsCCD3 (AF294900.1); *Drosophila melanogaster* DmCCD (AY121617.1); *Caenorhabditis elegans* CeCCD3 (AL110485.5) and CeCCD4 (AF098992.2).

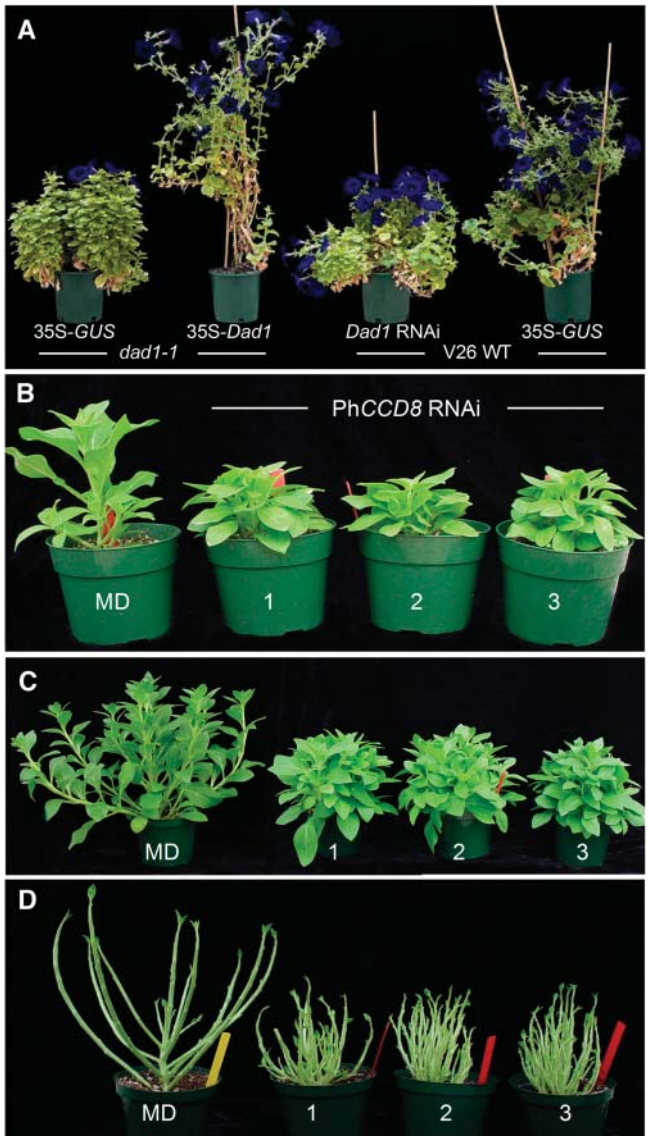

Figure 3. Complementation and Phenocopying of the *dad1-1* Mutant Phenotype.

(A) Complementation of *dad1-1* with *Dad1*/*PhCCD8* and phenocopying of the mutant phenotype in V26 with a *Dad1*/*PhCCD8* RNAi construct. Plants of similar ages with a control transgene are shown for comparison.
(B) Branching phenotypes of control (MD) and three independent *Dad1*/*PhCCD8* RNAi lines 8 weeks postgermination.
(C) The same plants as shown in **(B)** 12 weeks postgermination.
(D) Plants from **(C)** shown stripped of their leaves.

Stem cuttings (~8 cm in length) were also taken from sympodial shoots. After 6 weeks, wild-type cuttings showed the development of roots, but RNAi cuttings showed significantly less root development (Figure 6C). Paradoxically, mature RNAi plants developed adventitious roots around the lower stems at later stages of development (Figure 6D). Adventitious root formation was not observed on stems of wild-type MD or V26 plants. However, the formation of similar roots on the lower stems of *dad1-1* plants has been observed previously (Napoli, 1996).

The *Dad1*/*PhCCD8* Gene Is Expressed in Root and Stem Tissue

From micrograft analysis of the *dad1-1* mutant (Napoli, 1996; K.C. Snowden and C.A. Napoli, unpublished data), the *Dad1* gene was predicted to be expressed in root and stem tissue. *Dad1*/*PhCCD8* transcripts are present at very low levels and are not easily detectable by RNA gel blots in either V26 or MD plants. Expression of the gene was therefore examined using real-time PCR. We quantified the expression of the *Dad1*/*PhCCD8* gene in the leaves, stem, roots, and flowers (Figure 4B). *Dad1*/*PhCCD8* mRNA was detected at very low levels in the stem and leaves. The highest transcript levels were consistently detected in the roots representing 1.8×10^{-3}% total mRNA. Transcript levels decrease in roots segments further from the root tip, becoming

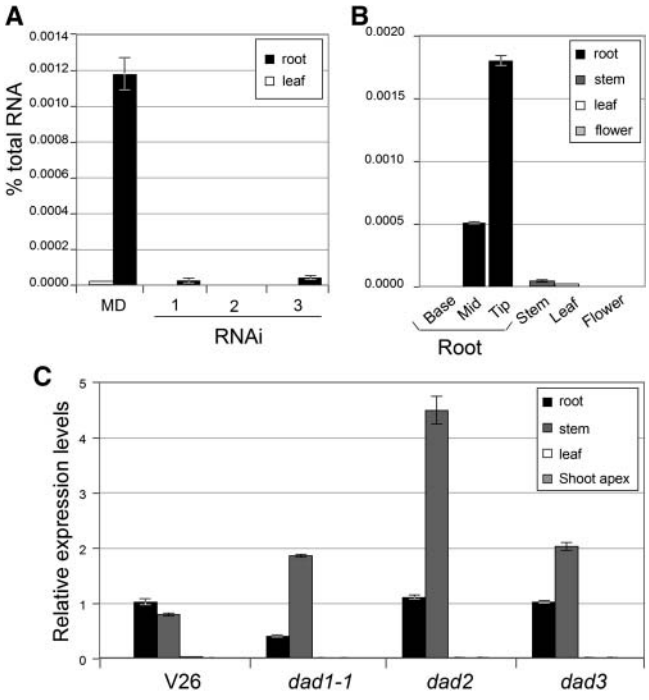

Figure 4. Expression of the *Dad1*/*PhCCD8* Gene in Petunia.

(A) *Dad1*/*PhCCD8* expression in roots and leaves of *Dad1*/*PhCCD8* RNAi plants as determined by TaqMan real-time RT-PCR.
(B) *Dad1*/*PhCCD8* expression in the tissues of wild-type MD plants as determined by TaqMan real-time RT-PCR. Roots were taken from 12-week-old plants separated into tip, middle, and base sections and analyzed independently. Stem tissue included the entire stem and nodes from mature flowering plants ranging from 30 to 35 cm in height from the base to the flower.
(C) Real-time RT-PCR analysis of *Dad1*/*PhCCD8* transcripts in 7-week-old V26 and *dad* mutant plants. The shoot apex sample included the apex of the plant, including leaves smaller than 1.5 cm in length. The root and stem samples included all root or stem tissue (except for that included in the shoot apex samples) from a pool of six plants. The plants were not flowering at the time of harvest.

Table 2. Dry Weight (in Grams) of MD Plants and Three Independent *PhCCD8* RNAi Lines at 12 Weeks Postgermination (Figures 3B and 3C)

Genotype	Leaf DW[a]	Mean	Stem DW	Mean	Total DW	Leaf/Stem Ratio
MD	8.67		4.68			
	8.05	8.00 ± 0.41	4.72	4.44 ± 0.26	12.44 ± 0.64	1.8
	7.27		3.93			
RNAi	5.72		1.85			
	5.60	5.66 ± 0.03	2.08	2.07 ± 0.13	7.73 ± 0.11	2.7
	5.66		2.29			

Standard errors were calculated from the means of three plants for each line.
[a] DW, dry weight.

undetectable in sections adjacent to the stem. *Dad1*/*PhCCD8* was not detected in flowers or in separated flower organs (Figure 4B; data not shown).

A difference in expression levels in MD was observed between experiments (Figures 4A and 4B). This was likely as a result of the use of a mix of midroot and root tip sections used to quantify the transcript levels in these samples.

We also used quantitative real-time PCR from a range of tissues from 7-week-old V26 plants and *dad1-1*, as well as the other petunia branching mutants (*dad2* and *dad3*), to detect expression of the *Dad1*/*PhCCD8* gene (Figure 4C). Expression was detected in root and stem tissue, and expression in leaf and shoot apex tissue was ~100-fold lower than expression in roots. We observed a difference in expression in stem tissue between the V26 and MD experiments (Figures 4B and 4C), which may have been as a result of the difference in age of the plants for each experiment. In a separate experiment, stem tissue from different positions of flowering V26 was analyzed for the expression of the *Dad1*/*PhCCD8* gene. In this experiment, expression of the gene was highest in lower positions of the stem and much lower in more apical sections of stem (both internodal and nodal tissue; data not shown).

Each of the *dad* mutants (*dad1-1*, *dad2*, and *dad3*) had increased expression of *Dad1*/*PhCCD8* in stem tissue relative to V26 (Figure 4C). The *dad1-1* mutant had decreased root expression of *Dad1*/*PhCCD8*, whereas the expression in the *dad2* and *dad3* mutants was unchanged in the roots. No change in gene expression was detected in the leaf and shoot apex samples.

DISCUSSION

Mutations in the CCD Gene Family Member *PhCCD8* Are Responsible for the Highly Branched Phenotype of *dad1* Mutants in Petunia

In this article, we have shown that mutations in the *Dad1*/*PhCCD8* gene are responsible for the highly branched *dad1* phenotype. Three mutant alleles of *dad1* were identified, and the *dad1-1* mutation was found to segregate with the mutant phenotype in two independent populations. Introduction of a cDNA copy of *Dad1* under the control of a constitutive promoter into *dad1* mutant plants was sufficient to restore the wild-type growth habit. Finally, we were able to phenocopy the *dad1* mutation by transforming wild-type plants with RNAi constructs that reduced endogenous *Dad1* gene expression. These results confirm that the *dad1* mutant phenotype results from a defect in the *Dad1*/*PhCCD8* gene.

The *Dad1* gene product is a member of a family that includes several enzymes that cleave double bonds in polyene chains. In plants, phylogenetic analysis of the gene family reveals multiple distinct clades. One large clade contains the NCEDs, enzymes that catalyze the first committed step in production of the plant hormone ABA (Schwartz et al., 1997; Tan et al., 1997). A second clade contains the *Dad1* gene as well as the orthologs *MAX4*/*CCD8* and *RMS1* (Sorefan et al., 2003; M. Auldridge and H.J. Klee, unpublished data). A third distinct plant clade contains the Arabidopsis *MAX3*/*CCD7* gene, also involved in the control of branching (Booker et al., 2004). The MAX3/CCD7 enzyme is a CCD, having the capacity to cleave multiple carotenoid substrates at the 9,10 or 9′,10′ double bonds (Booker et al., 2004).

Within the *Dad1* clade, only CCD8/MAX4 has been characterized with respect to biochemical activity. When β-carotene was provided as a substrate, this enzyme worked together with CCD7/MAX3 to produce 13-apo-β-carotenone, a C_{18} apocarotenoid (Schwartz et al., 2004). We have shown that CCD7/MAX3 is a dioxygenase that recognizes and cleaves multiple linear and cyclic carotenoid substrates at the 9,10 position (Booker et al., 2004). Thus, although CCD8/MAX4 is capable of producing 13-apo-β-carotenone, it is not certain what the biologically active product(s) is. However, it is clear that Dad1 is a CCD whose action is essential for subsequent movement of a compound from the roots to the shoot. The genetic and biochemical evidence in Arabidopsis (Sorefan et al., 2003; Booker et al., 2004) and petunia (K.C. Snowden, C.A. Napoli, and B.J. Janssen, unpublished data) supports a model in which CCD8 and CCD7

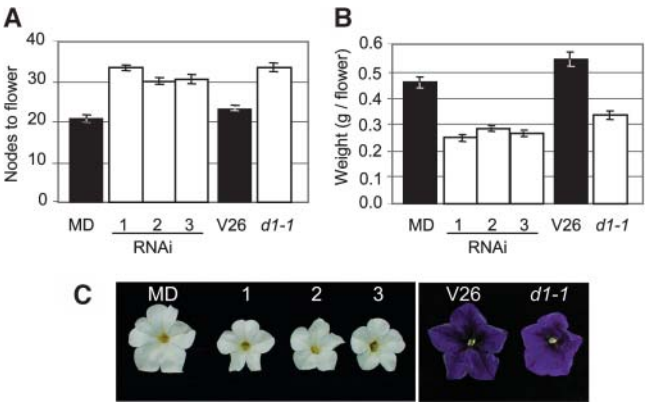

Figure 5. Flowering-Associated Phenotypes in *Dad1*/*PhCCD8* Loss-of-Function Lines.

(A) Number of nodes before the terminal flower in *Dad1*/*PhCCD8* RNAi lines and *dad1-1* compared with wild-type controls (MD and V26).
(B) Flower weight of *Dad1*/*PhCCD8* RNAi lines and *dad1-1* compared with wild-type controls.
(C) Flowers from *Dad1*/*PhCCD8* RNAi lines and *dad1-1* compared with the wild type.

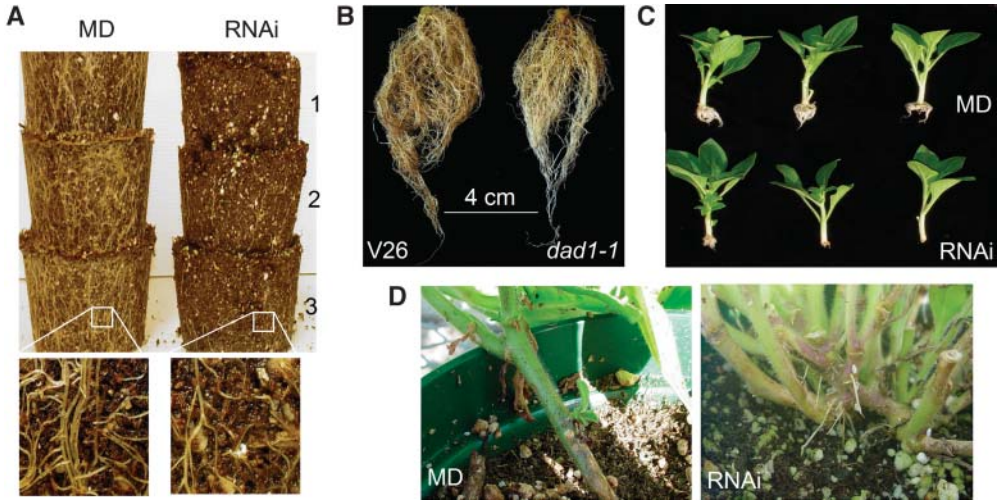

Figure 6. Root Phenotypes Associated with Loss of *Dad1*/*PhCCD8*.

(A) Roots of wild-type (MD) and *Dad1*/*PhCCD8* RNAi plants 12 weeks postgermination.
(B) Roots of wild-type (V26) and *dad1-1* plants 13 weeks postgermination.
(C) The development of roots on cuttings from MD and *Dad1*/*PhCCD8* RNAi lines after 6 weeks.
(D) Adventitious roots developing on the lower stems of a *Dad1*/*PhCCD8* RNAi line but not on wild-type (MD) stems.

act in the same pathway to produce a novel, graft-transmissible apocarotenoid hormone either as sequential steps, where the intermediate is not mobile, or at the same step. The conservation of the CCD8 gene and the mutant phenotypes between petunia, pea, and Arabidopsis indicates that branch development is controlled by a similar mobile signaling molecule, which in turn suggests that the mechanism of control of branch development may be widely conserved.

Phenotypic Analysis of the *dad1* Alleles Suggests That Partial Loss of Function of the DAD1 Protein Is Possible

The *dad1-1* allele is predicted to produce a truncated protein that is unlikely to have any biological activity because it is missing amino acids that are completely conserved in all of the CCDs. The *dad1-1* mutant allele produces branches at every node up to the 10th node and exhibits reduced height, delayed flowering, and reduced leaf senescence (Figures 1A and 1B; Snowden and Napoli, 2003). The *dad1-2* allele has a single amino acid substitution that replaces a Tyr at amino acid 456 with a Ser. This amino acid is highly conserved, being either a Phe or a Tyr in every member of the Arabidopsis gene family, and substitution of Ser apparently compromises the activity of the enzyme. This amino acid substitution results in a phenotype intermediate between *dad1-1* and the wild type for some but not all traits. An intermediate phenotype has not been reported for any alleles of the *max4* or *rms1* mutants (Sorefan et al., 2003). These results suggest that, in *dad1-2* mutants, the translocated substance is present at reduced levels and affects the different developmental processes to varying degrees. However, we cannot exclude the possibility that the Dad1/PhCCD8 protein acts on multiple substrates and the *dad1-2* mutation alters substrate specificity. The phenotype of *dad1-3* plants is almost indistinguishable from the wild type, suggesting that inclusion of an additional three amino acids in this region of the protein has a minimal effect on the biological activity of the protein.

The *dad1-1* Mutation Was Caused by Insertion of a Novel Transposon (*Dot*)

Sequencing of the *dad1-1* allele revealed the presence of a 1.1-kb insertion in exon 2 that was not present in the wild-type gene. This was unexpected because the *dad1-1* allele was generated by EMS mutagenesis (Napoli and Ruehle, 1996). This insertion has some features characteristic of a transposon: at each end of the insertion is a 10-bp direct repeat of the *Dad1* sequence, and the insertion contains a highly repetitive structure (Figure 2D). In addition, DNA gel blot analysis using the insertion sequence as a probe revealed multiple copies of related sequences in the petunia genome, as would be expected for an active transposon. However, no terminal repeats (inverted or

Table 3. Fresh Weight of Root and Shoot (All Stem and Leaf Tissue) of V26 and *dad1-1* Mutants at 9 and 13 Weeks Postgermination (Figure 6B)

Tissue	V26	*dad1-1*	LSD
Root FW (g)[a]	2.24	1.60	0.480
Shoot FW (g)	38.5	38.7	7.97

Data was analyzed by two-way ANOVA using the GenStat (version 7) statistical software package. Values given are means. No interactions were detected between genotype and age of plants at harvest. LSD, least significant differences of means (5% level). If means differ by more than the LSD shown, then they are significantly different.
[a] FW, fresh weight.

direct) could be found. No instability of the *dad1-1* mutant had been observed over more than 12 generations and thousands of individual plants grown. However, when seeds of the *dad1-1* mutant were treated with EMS to identify second-site suppressors of the *dad1-1* mutation, the *dad1-3* revertant allele was isolated. This mutagenesis appears to have resulted in excision of the insertion found in the *dad1-1* allele, presumably as a result of activation of a transposable element, perhaps in response to genomic stress (McClintock, 1984; Kunze, 1996). Sequencing of the *Dad1* gene in this revertant allele revealed excision of the 1.1-kb insertion and the presence of a 9-bp footprint corresponding to part of the insertion sequence and the remaining target site duplication seen in the *dad1-1* sequence. The target site duplication, combined with the EMS-induced excision of this 1.1-kb insertion and the presence of the footprint, provides strong evidence that the insertion sequence found in the *dad1-1* allele is a transposon, which we have named *Dot*. The identification of an additional transposon in petunia may prove useful for isolation of genes in the future, particularly because transposition may be inducible by EMS mutagenesis.

The lack of any terminal repeat structures in an active transposon is unusual. The structure of this insertion element suggests that it would form a unique transposon class. Many characterized transposon families (e.g., *En*/*Spm* or *Ac*/*Ds*) have repetitive elements, particularly in the subterminal regions. However, the transposon found in the *dad1-1* allele has a different structure. The major repetitive elements are located in the middle of the element, with multiple degenerate copies of an 18-bp palindrome. Searches within sequence databanks have not found other sequences with homology to this element. Although the element does contain some ORFs, all those that are larger than 30 amino acids are found within the middle repetitive region or within the regions with high TC or GA composition. None of the putative ORFs present within the element has any homology to known proteins. It is likely that if transposition of this element requires protein(s), are derived from elsewhere in the genome (i.e., this element is probably nonautonomous in the manner of transposons such as *Ac*/*Ds* [Kunze, 1996]).

Axillary Meristems Are Produced Early in Wild-Type V26 but Do Not Develop into Branches

Scanning electron microscopy of cotyledonary axils from both V26 and *dad1-1* mutants revealed that, in wild-type plants, cotyledon axil meristems and axillary shoots appear to form at an earlier stage of development than in *dad1-1*. However, these shoots do not continue growth to form branches in the wild type. By contrast, branches are formed from both cotyledonary nodes in *dad1-1*, yet scanning electron micrographs showed no detectable meristem development for the majority of the *dad1-1* axils at the stage that was examined. One question is whether the meristems formed in the cotyledonary nodes of *dad1-1* mutants are fundamentally different from normal axillary meristems that develop in the wild type. It may be that *dad1-1* mutants fail to form normal axillary meristems at all, and the branches that do form may result from adventitious meristems that form as a result of an abnormal signal present in the mutant. Alternatively, meristem formation may simply be delayed in the *dad1-1* mutant, but, once initiated, shoot growth proceeds without dormancy. This result contrasts with the observation of the *max1* and *max2* mutants, in which timing of meristem initiation is not changed but development of primordia by the axillary meristem is advanced relative to the wild type (Stirnberg et al., 2002). Thus, it may be that the imposition of dormancy of axillary meristems occurs at different stages in petunia and Arabidopsis and warrants further investigation.

The *Dad1* Gene Is Involved in Leaf Senescence

While examining the branching phenotype of the *dad1* mutants, we observed that leaf senescence was delayed in *dad1-1* and *dad1-2* mutants, with *dad1-2* having an intermediate phenotype. The difference observed between *dad1-1* and the wild type may be a consequence of the difference in flowering time between these two genotypes. However, the *dad1-2* allele also shows delayed leaf senescence without any alteration in flowering time. A relationship between branching phenotype and senescence has been shown previously for the *oresara9* (*ore9*)/*max2* mutant of Arabidopsis (Woo et al., 2001; Stirnberg et al., 2002). This mutant was originally isolated in a screen for mutants with delayed leaf senescence (Oh et al., 1997). Subsequent positional cloning of the *ore9* gene (Woo et al., 2001) showed that it is a member of the Leu-rich repeat–type F-box gene family, involved in ubiquitin-dependent degradation of proteins. Positional cloning of the branching mutant *max2* (Stirnberg et al., 2002) identified the same F-box gene, identifying a linkage between branch development and leaf senescence.

The finding that mutations in *Dad1* also affect both branching and leaf senescence suggests that the *Dad1*/*PhCCD8* and *ORE9*/*MAX2* genes could affect the same signaling pathway. A direct interaction between the F-box protein and Dad1/PhCCD8 protein is unlikely because ubiquitin-mediated degradation of Dad1/PhCCD8 by ORE9/MAX2 would result in opposite phenotypes for mutations in these genes. Further, Dad1/PhCCD8 is likely to be located in the plastid, based on its homology to the chloroplast-localized Arabidopsis ortholog AtCCD8 (M. Auldridge and H.J. Klee, unpublished data). Ubiquitin-dependent protein turnover is not believed to occur in plastids (Beers et al., 1992).

It is possible that the translocated hormone has a role in initiation of leaf senescence. The apocarotenoid hormone ABA has been shown to promote leaf abscission, flower senescence, and senescence of excised leaf discs (Smart, 1994), and the enzymes from the NCED clade of the gene family have been shown to be responsible for the first committed step in ABA production (Schwartz et al., 1997). Thus, it seems reasonable to suggest that the Dad1/PhCCD8 protein is involved in production of a similar compound that has a role in leaf senescence. However, the *ore9*/*max2* mutant has a reduced response to inducers of senescence, including ABA, methyl jasmonate, and ethylene (Woo et al., 2001), suggesting that *ore9*/*max2* acts at a point downstream or independent of the ABA senescence signal. Furthermore, the role of cytokinin in leaf senescence (Gan and Amasino, 1995) and branch development (Napoli et al., 1999) suggests that the role of *Dad1*/*PhCCD8* in leaf senescence may be indirect.

Loss of *Dad1* Expression Results in Reduced Root Development

In transgenic MD plants expressing an RNAi construct and in the *dad1-1* mutant, root mass is reduced. In RNAi lines, the formation of adventitious roots on cuttings also is inhibited. By contrast, in both wild-type plants transformed with an RNAi construct (Figure 6D) and in *dad1-1*, adventitious roots are observed on the lower portions of the stems (Napoli, 1996). Whether adventitious root formation is a consequence of reduced root growth is not clear. It also is not clear whether the *Dad1* gene product has a normal role in root development, or whether the altered root growth observed is a consequence of a build up of the substrate of the *Dad1* gene product or even a consequence of altered shoot growth. We do not, however, believe that the shoot morphology is simply a result of reduced root mass because when *dad1-1* mutant scions are grafted onto wild-type roots, the presence of *dad1-1* mutant roots above the graft union induces the mutant branching phenotype despite the presence of a wild-type (normal-sized) root mass.

Expression of *Dad1*/*PhCCD8* Suggests That the Gene Is under Feedback Control

The expression of the *Dad1*/*PhCCD8* gene observed in roots and stems of petunia plants is consistent with a role in control of a graft-transmissible substance that can alter growth of axillary branches. The increased levels of expression in the stems of *dad1-1*, *dad2*, and *dad3* mutants relative to the wild type are indicative of a feedback control mechanism that is responding to a change in the amount or detection of a branching signal. This increased expression is not seen in the root tissue of the *dad* mutants, suggesting that the feedback mechanism is restricted to the stem tissue, and expression in the roots may be independently controlled. Although the level of *Dad1*/*PhCCD8* RNA in the roots of the *dad2* and *dad3* mutants is unchanged, it is significantly lower in the roots of the *dad1-1* mutant than in the wild type. The insertion in the *dad1-1* mutant may lead to mRNA instability and a high level of mRNA turnover. In *dad1-1* stems, any increase in mRNA turnover may be masked by positive feedback.

The Role of *Dad1*/*PhCCD8* in Branch Signaling

Observations made in petunia by Napoli (1996) suggested that a mobile signal molecule is transported from the roots acropetally to the axillary meristems, where branch development occurs. From graft analysis, such a signal must be produced in the roots and transported across graft unions. These observations in petunia have been replicated in pea (Beveridge et al., 1994, 2000; Foo et al., 2001) and Arabidopsis (Turnbull et al., 2002). Interstock grafts in which a small section of wild-type stem is inserted above *dad1* mutant roots and below *dad1* mutant scion also revert the mutant scion to wild-type phenotype (Napoli, 1996). This result indicates that the *Dad1*/*PhCCD8* gene product is also present and active in stem tissue, which we have confirmed by expression analysis (Figure 4C). Because only a small piece of wild-type stem interstock tissue is required for reversion, the *Dad1*/*PhCCD8* gene product must be active to a high enough level to produce the wild-type phenotype.

Although these observations strongly suggest a mobile signal that is acted upon in some way by the *Dad1*/*PhCCD8* gene product, they do not define whether the mobile signal is a repressor or promoter of branching. Two possibilities exist. First, the *Dad1*/*PhCCD8* gene product acts to produce or transport a repressor of branching, and in the absence of *Dad1*/*PhCCD8*, lack of this repressor results in branching. Alternatively, the substrate of the *Dad1*/*PhCCD8* gene product (possibly subsequently processed) is a promoter of branching that is processed or in some way inactivated by the *Dad1*/*PhCCD8* gene product. In the absence of *Dad1*/*PhCCD8,* this promoter of branching is transported to the shoot and induces branching. However, in petunia, when *dad1* mutant scions are grafted onto wild-type rootstocks and *dad1* mutant roots form above the graft, the plant does not revert to the wild type (Napoli, 1996; K.C. Snowden, unpublished data). When these roots are removed, subsequent nodes revert to the wild type and do not branch. This result is consistent with the presence of a promoter of branching that is produced from *dad1* mutant roots and transported to the shoot, where branches are induced. These two possibilities are not mutually exclusive. The *Dad1*/*PhCCD8* gene product may produce an inhibitor of branching in addition to the substrate being a promoter of branching. However, in the grafts described above, this putative inhibitor is not sufficient to prevent branch development in the presence of the promoter of branching being produced by the *dad1* mutant roots. If indeed the *Dad1*/*PhCCD8* gene product converts a promoter of branching into an inhibitor, it is possible that in other species the balance between promotion and inhibition of branch development is altered.

METHODS

Genetic Stocks and Plant Growth Conditions

Inbred cv MD petunia (*Petunia axillaris* × [*P. axillaris* × *Petunia integrifolia*]) plants were grown under greenhouse conditions with a day/night temperature regime of 25°C/18°C in commercial potting medium (Fafard 2B; Conrad Fafard, Agawam, MA) in 15-cm, 1.5-L pots and were fertilized at each irrigation with 150 mg L^{-1} nitrogen from 15:7:14.1 soluble fertilizer (Peter's Fertilizer Products, Fogelsville, PA).

Petunia (*Petunia hybrida*) Vilm inbred genetic stock V26 and the *dad* mutants derived from V26 (Napoli and Ruehle, 1996) were grown under greenhouse conditions with a minimum/maximum temperature regime of 20°C to 30°C and a minimum of 12 h light, supplemented when necessary. Plants for RNA isolation and the characterization of the *dad1* alleles were grown in commercial potting medium (Dalton's potting mix; Matamata, New Zealand) in six-packs (100-mL size); transgenic plants were initially grown in 400-mL pots and then transferred to 1.5-liter pots after 6 to 8 weeks. All plants were fertilized at each irrigation with 80 mg L^{-1} nitrogen, 80 mg L^{-1} phosphorus, and 60 mg L^{-1} potassium (from Wuxal Super 8-8-6 plus micro liquid fertilizer; Aglukon, Düsseldorf, Germany).

Alleles of *dad1* were grown until they were 12 weeks of age. Nodes were recorded and branches defined as by Snowden and Napoli (2003).

Gene Isolation and Vector Construction

RNA was isolated from combined root and stem tissue of V26 using an RNeasy plant mini kit (Qiagen, Hilden, Germany). cDNA was synthesized

using Superscript II reverse transcriptase (Invitrogen, Carlsbad, CA) and used as a template for PCR using primers designed from the amino acid sequence of the *Arabidopsis thaliana MAX4*, pea (*Pisum sativum*) *RMS1*, and rice (*Oryza sativa*) CCD8 genes, forward primer 5′-TTCCGGCATCTCTTCGACGGCTAC-3′ and reverse primer 5′-GGATCCAGCAACCATGCAAGCC-3′. This PCR was used as template in a second nested PCR using redundant primers, forward 5′-GTIATGTGYYTNACNGARAC-3′ and reverse 5′-TAIGGNARICCRTANGGRAA-3′. A 1-kb fragment was isolated and cloned into the pGEM-T Easy vector (Promega, Madison, WI). Sequence of this clone was used to design primers for inverse PCR from genomic DNA. Inverse PCR (Snowden and Napoli, 1998) from V26 genomic DNA was used to isolate the 5′ and 3′ ends of the gene. After obtaining a full-length sequence for the gene, proofreading PCR was used to isolate overlapping fragments of the gene from V26 and *dad1*. PCR products were sequenced directly to obtain confirmed sequences of the gene and the mutants.

To generate a vector for the overexpression of *Dad1*/*PhCCD8*, a cDNA clone containing the full ORF of *Dad1*/*PhCCD8* was generated using primers 5′-CAAACTTAGCAGACCATAAAGAGTGCAC-3′ and 5′-GTCTGGGATGTGAGGTAACTA-3′ and ligated into pGEM-T Easy. PCR amplification was performed using this clone as template with primers SP33 (5′-attB2-CCGGGCCCCCCCTCGAG-3′) and SP30 (5′-attB1-CCCCGGGCTGCAGGAATTC-3′). The resulting 1667-bp PCR amplification product was recombined via an attB × attP Gateway reaction with pDONR201 to generate pENTRY_DAD1. A Gateway attL × attR reaction with pENTRY_DAD1 and the pHEX1 destination vector was performed to generate pHEX1S_DAD1. All Gateway reactions were performed as recommended by the manufacturer (Invitrogen). pHEX1 is a Gateway-adapted version of the pART7/pART27 plant transformation vector system (Gleave, 1992) with the Gateway 1711-bp RfA cassette cloned into the *Sma*I site between the CaMV 35S promoter and the octopine synthase transcriptional terminator (35S-attR2-ccdB-CmR-attR1-ocs3′).

To generate the *Dad1*/*PhCCD8* RNAi vector used in the V26 experiments, a 388-bp region of the *Dad1*/*PhCCD8* ORF (corresponding to bases 435 to 822 of the ORF) was PCR amplified from V26 using primers oKCS1 (5′-attB1-ATCTGATGCATACAAGGCAG-3′) and oKCS2 (5′-attB2-CCTCTCATTTGTTCCTGCTTC-3′). The resulting 437-bp PCR product was recombined via an attB × attP Gateway reaction with pDONR201 to generate pENTRY_DAD1(ko). A Gateway attL × attR reaction with pENTRY_DAD1(ko) and the destination vector pTKO2 was performed to generate pTKO2S_DAD1.

To construct pTKO2, the 443-bp intron from the 5′ untranslated region (UTR) of the Arabidopsis Columbia Actin2 (ACT2) gene was PCR amplified from genomic DNA using primers INT1 (5′-GCCCGTGGATCCCTCGAGTCCGGAACTAGTCTGCAGGTAATAGGAACTTTCTGGAT-3′; underlined regions denote homology to ACT2) and INT2 (5′-GCCCGTAAGCTTGTCGACACCGGTGCTAGCATGCATCCTGCAAACACACAAAAAGAG-3′). A 658-bp region of the 3′ UTR and transcriptional terminator of the Arabidopsis ACT2 gene was PCR amplified from Columbia genomic DNA using primers ACT3-1 (5′-GGGCCTAAGCTTGAGGCTCTCAAGATCAAAGG-3′) and ACT3-2 (5′-GGGCCTGGTACCGCGGCCGCACTTTTTGGAATCAAGATGTA-3′). A triple-enhanced version of the CaMV 35S promoter (Que et al., 1997) was PCR amplified from pCHS3061 using primers 3×35S-1 (5′-GGGCCGTATCTAGAATTCAATCCCACCAAAACC-3′) and 3×35S-2 (5′-GCAAAGAGCTCTTATACTCGAG-3′). The 515-bp ACT2 intron PCR product was cloned as a *Bam*HI-*Hin*dIII fragment into pBluescript SK− (Stratagene, La Jolla, CA). The 693-bp ACT2 transcriptional terminator PCR product was then cloned distal to the intron as a *Hin*dIII-*Kpn*I fragment. Subsequently, the 942-bp CaMV 35S promoter PCR product was cloned proximal to the intron as an *Xba*I-*Xho*I fragment. This created pPAN1 with an organizational structure of 35S-intron-ACT3′. To convert pPAN1 into a Gateway compatible vector, the 1711-bp Gateway RfA cassette (attR1-CmR-ccdB-attR2) was first cloned into the *Pvu*II site of pSP72 (Promega) and then excised as a *Xho*I-*Xba*I fragment and cloned into *Sal*I-*Nhe*I sites of pPAN1, placing the RfA cassette between the ACT2 intron and transcriptional terminator. To reduce sequence duplication in the final vector, a *Bam*H1 deletion was then produced, removing 703 bp from the RfA cassette, including the entire chloramphenicol resistance gene. A second intact RfA cassette was then cloned as an *Xho*I-*Xba*I fragment into the *Xho*I-*Spe*I sites, placing the RfA cassette between the 35S promoter and the intron and in the inverse orientation to the first RfA cassette introduced. The resulting vector, referred to as pTKO1, has an organizational structure of 35S-attR1-Cm^R-*ccd*B-attR2-intron-attR2-*ccd*B-attR1-Act2. pTKO1 was digested with *Xba*I, followed by a partial *Not*I digestion, and the 4838-bp Gateway-adapted 35S-intron-ACT2 3′ cassette was cloned into *Spe*I-*Not*I sites of the plant transformation vector pART27 (Gleave, 1992), generating pTKO2. The presence of the two Gateway RfA-derived cassettes, in an inverse orientation, facilitates the introduction of two copies of a selected gene fragment into the vector in a single Gateway attL × attR reaction, generating an inverted repeat of the gene fragment, flanking the intron sequence. When transcribed, this produces a self-complementary RNA able to efficiently induce gene silencing.

A 2-kb fragment of *PhCCD8* genomic sequence from MD from positions 359 bp to 1462 bp of the coding sequence was cloned using degenerate forward (5′-GAGACCACGCTTCCGGCATCTCTTYGACGGSTAC-3′) and reverse (5′-AAYTTCCCAATACTCTGACTAA-3′) primers corresponding to the GDHDFRHLFDGY and NFPNALSK conserved protein sequences of the AtCCD8 and PsRMS1 orthologs. The remaining sequence was recovered by Genewalker (BD Biosciences, Palo Alto, CA). A 643-bp partial coding sequence of *PhCCD8* from positions 359 to 1002 was recovered by PCR with the addition of an *Asc*I restriction site at the 3′ end. A second 316-bp partial cDNA fragment from positions 359 to 675 was recovered by PCR with an *Asc*I site at the 3′ end. The two fragments were ligated at the *Asc*I site and introduced into the pDESTOE vector (Booker et al., 2004) by recombination from the pENTR/D vector (Invitrogen). The *Dad1*/*PhCCD8* RNAi construct used in transgenic MD plants was under transcriptional control of the *Figwort mosaic virus* promoter (Richins et al., 1987) followed by the *nos* 3′ terminator.

Transgenic petunia plants were produced using Agrobacterium-mediated transformation of 5-week-old petunia seedlings or tissue culture–grown plants according to the method of Jorgensen et al. (1996). Introduction and inheritance of the transgenes were confirmed by PCR using primers specific for the neomycin phosphotransferase II marker gene. All phenotypic characterizations of transgenic RNAi lines were performed on PCR-positive T1 plants.

Scanning Electron Microscopy

V26 and *dad1-1* seedlings for scanning electron microscopy analysis were germinated and grown on 0.5× MS (including vitamins; Duchefa, Haarlem, The Netherlands) plates, supplemented with 15 g L^{-1} sucrose, until they had one visible true leaf. Seedlings were harvested and fixed in 2.5% glutaraldehyde in 0.1 M potassium phosphate buffer, pH 7.2, under vacuum for 1 h and then stored overnight at 4°C. After fixation, tissue was dehydrated in a graded ethanol series and then dried with a Bal-Tec CPD 030 critical point drier (Balzers, Liechtenstein). Seedlings were secured to stubs with carbon tabs and sputter coated with gold using a Polaron E5100 (Quorum Technologies, Newhaven, UK). Specimens were viewed with a Philips 505 scanning electron microscope (Eindhoven, The Netherlands) at 15 kV.

Quantitative RT-PCR

Total RNA was isolated from tissues using the RNeasy plant mini kit (Qiagen). RNA from V26 was treated with DNase (using the Ambion DNA-free kit; Austin, TX). Concentration and purity of RNA was checked

using an Agilent 2100 bioanalyzer before and after DNase treatment. Three independent reverse transcription reactions (containing 1.5 μg of RNA, 3.5 μM of poly(dT)$_{23}$V primer, 1 mM dNTP, 10 mM DTT, 1× first-strand RT buffer, and 200 units of Superscript III RT [Invitrogen]) were incubated at 55°C for 1 h and then pooled. Primers were designed for *Dad1*/*PhCCD8* (forward 5′-GTGGCAAGTGTAGAAGTTCC-3′, reverse 5′-TCAGCGCTATGCTCACAGC-3′) and the control genes ACT2 (forward 5′-CCTGATGAAGATCCTCACCGA-3′, reverse 5′-CAAGAGCCACATAG-GCAAGCT-3′), EF1α (forward 5′-TGTTCTCTGCCTTGTATGTCTGG-3′, reverse 5′-TCAAAAGAGGCAGGCAGACAG-3′), and Histone H4 (forward 5′-ATACGCTTGCACCCACCCCTA-3′, reverse 5′-GGAGGAGCTAAAC-GACACCG-3′). At least three replicate real-time PCR reactions were set up for each primer pair. An aliquot of each pooled cDNA (1/300th) was used as template for each reaction (containing 1× Platinum Taq reaction buffer [Invitrogen], 0.1 mM dNTP, 1.5 mM $MgCl_2$, 0.2 mM of each primer, 0.1× SYBR Green I dye [Molecular Probes, Eugene, OR], and 0.5 units of Platinum Taq polymerase in a total volume of 20 μL). Reaction mixtures were denatured for 2 min at 94°C and then amplified for 40 cycles (15 s at 94°C, 30 s at 59°C, 20 s at 72°C), followed by a dissociation stage (15 s at 95°C, 30 s at 60°C with a slow ramp to 15 s at 95°C). Amplification and expression quantification was performed using the ABI PRISM 7900 HT sequence detection system (Applied Biosystems, Foster City, CA). Data were analyzed with the SDS 2.0 software (Applied Biosystems) using the OBT (Outlier, Baseline, Threshold) principle. Relative expression was calculated using the comparative cycle threshold method (Pfaffl, 2001) with normalization of data to the geometric average of the internal control genes (Vandesompele et al., 2002). PCR efficiency for the amplicon was estimated using the absolute fluorescence (window of linearity) method (Ramakers et al., 2003), using data from the exponential phase of each individual amplification plot.

RNA samples from MD were treated with RNase-free DNase (Qiagen) and purified using Qiagen minicolumns. Samples were checked for DNA contamination by TaqMan real-time RT-PCR in a reverse-minus transcription reaction. Concentration and purity of total plant RNA was determined by spectrophotometric analysis. The quantification was verified for all RNA samples in each experiment by formaldehyde agarose gel electrophoresis and visual inspection of rRNA bands upon ethidium bromide staining. TaqMan one-step real-time RT-PCR was performed as recommended by the manufacturer (Perkin-Elmer Applied Biosystems, Foster City, CA). All reactions contained 1× TaqMan buffer (Perkin-Elmer Applied Biosystems); 5 mM $MgCl_2$; 200 μM dATP, 200 μM dCTP, and 200 μM dGTP; 400 μM dUTP; 0.625 units of AmpliTaq Gold polymerase; and 0.25 units of MultiScribe RNA reverse transcriptase and RNase inhibitor in a 25-μL volume. Reverse transcription was performed using 250 ng of total RNA, each gene-specific primer at 500 nM (forward, 5′-AATTATTCTCAGGTGCATCGTTGA-3′; reverse, 5′-GCAAACAACTCGGCCATCA-3′), and 250 nM TaqMan probe (5′-CGATAACGCGAATACAGGAGTCGTTA-3′). Reaction mixtures were incubated for 30 min at 48°C for reverse transcription, 10 min at 95°C, followed by 40 amplification cycles of 15 s at 95°C/1 min at 60°C. Samples were quantified in the GeneAmp 5700 sequence detection system (Perkin-Elmer Applied Biosystems). Absolute mRNA levels were quantified against a standard curve of tritiated in vitro-transcribed sense-strand RNAs. Primers and probes used in the TaqMan real-time quantitative RT-PCR assay were designed using PRIMER EXPRESS software (Applied Biosystems). All probes were labeled at the 5′ with fluorescent reporter dye 6-carboxyfluorescein and at the 3′ with black hole quencher-1 from Integrated DNA Technologies (Coralville, IA; Bernacchi and Mély, 2001).

Sequence data from this article have been deposited with the EMBL/GenBank data libraries under accession numbers AY743219, AY745251, and AY746977.

ACKNOWLEDGMENTS

This work was supported by Marsden and FoRST grants to K.S. and by National Science Foundation Grant IBN-0115004 to H.K. This is publication R-10632 of the Florida Agricultural Experiment Station. We thank Carolyn Napoli for helpful discussions and generation of the *dad1-3* allele and Toshi Foster and Paul Sutherland for assistance with scanning electron microscopy.

Received September 15, 2004; accepted December 5, 2004.

REFERENCES

Altschul, S.F., Gish, W., Miller, W., Myers, E.W., and Lipman, D.J. (1990). Basic local alignment search tool. J. Mol. Biol. **215,** 403–410.

Beers, E., Moreno, T., and Callis, J. (1992). Subcellular localization of ubiquitin and ubiquitinated proteins in *Arabidopsis thaliana*. J. Biol. Chem. **267,** 15432–15439.

Bell, A.D. (1991). Plant Form: An Illustrated Guide to Flowering Plant Morphology. (Oxford: Oxford University Press).

Bernacchi, S., and Mély, Y. (2001). Exciton interaction in molecular beacons: A sensitive sensor for short range modifications of the nucleic acid structure. Nucleic Acids Res. **29,** E62–2.

Beveridge, C.A. (2000). Long-distance signalling and a mutational analysis of branching in pea. Plant Growth Regul. **32,** 193–203.

Beveridge, C.A., Ross, J.J., and Murfet, I.C. (1994). Branching mutant *rms-2* in *Pisum sativum* (grafting studies and endogenous indole-3-acetic acid levels). Plant Physiol. **104,** 953–959.

Beveridge, C.A., Symons, G.M., and Turnbull, C.G.N. (2000). Auxin inhibition of decapitation-induced branching is dependent on graft-transmissible signals regulated by genes *Rms1* and *Rms2*. Plant Physiol. **123,** 689–697.

Beveridge, C.A., Weller, J.L., Singer, S.R., and Hofer, J.M.I. (2003). Axillary meristem development. Budding relationships between networks controlling flowering, branching and photoperiod responsiveness. Plant Physiol. **131,** 927–934.

Booker, J., Auldridge, M., Wills, S., Klee, H.J., and Leyser, O. (2004). MAX3 is a carotenoid cleavage dioxygenase required for the synthesis of a novel plant signalling molecule. Curr. Biol. **14,** 1232–1238.

Bouvier, F., Dogbo, O., and Camara, B. (2003a). Biosynthesis of the food and cosmetic plant pigment bixin. Science **300,** 289–291.

Bouvier, F., Suire, C., Mutterer, J., and Camara, B. (2003b). Oxidative remodeling of chromoplast carotenoids: Identification of a carotenoid cleavage dioxygenase *CsCCD* and *CsZCD* genes involved in Crocus secondary metabolic biogenesis. Plant Cell **15,** 47–62.

Felsenstein, J. (2004). PHYLIP (Phylogeny Inference Package), Version 3.6b. (Seattle: University of Washington).

Foo, E., Turnbull, C.G., and Beveridge, C.A. (2001). Long-distance signaling and the control of branching in the *rms1* mutant of pea. Plant Physiol. **126,** 203–209.

Gan, S., and Amasino, R.M. (1995). Inhibition of leaf senescence by autoregulated production of cytokinin. Science **270,** 1986–1988.

Gleave, A. (1992). A versatile binary vector system with a T-DNA organisational structure conducive to efficient integration of cloned DNA into the plant genome. Plant Mol. Biol. **20,** 1203–1207.

Gollapalli, D.R., Maiti, P., and Rando, R.R. (2003). RPE65 operates in the vertebrate visual cycle by stereospecifically binding all-*trans*-retinyl esters. Biochemistry **42,** 11824–11830.

Hallé, F. (1999). Ecology of reiteration in tropical trees. In The Evolution of Plant Architecture, M.H. Kurmann and A.R. Hemsley, eds (Surrey, UK: Royal Botanic Gardens, Kew), pp. 93–107.

Jorgensen, R.A., Cluster, P.D., English, J., Que, Q., and Napoli, C.A. (1996). *Chalcone synthase* cosuppression phenotypes in petunia flowers: Comparison of sense vs. antisense constructs and single-copy vs. complex T-DNA sequences. Plant Mol. Biol. **31,** 957–973.

Kamoda, S., and Saburi, Y. (1993a). Cloning, expression and sequence analysis of a lignostilbene-α,β-dioxygenase gene from *Pseudomonas paucimobilis* TMY1009. Biosci. Biotechnol. Biochem. **57,** 926–930.

Kamoda, S., and Saburi, Y. (1993b). Structural and enzymatical comparison of lignostilbene-α,β-dioxygenase isozymes, I, II and III, from *Pseudomonas paucimobilis* TMY1009. Biosci. Biotechnol. Biochem. **57,** 931–934.

Kunze, R. (1996). The maize transposable element *Activator* (*Ac*). Curr. Top. Microbiol. Immunol. **204,** 161–194.

Lindqvist, A., and Anderson, S. (2002). Biochemical properties of purified recombinant human β-carotene 15,15'-monooxygenase. J. Biol. Chem. **277,** 23942–23948.

Maddison, D.R., and Maddison, W.P. (2000). MacClade 4: Analysis of Phylogeny and Character Evaluation, Version 4.0. (Sunderland, MA: Sinauer Associates).

Mata, N.L., Moghrabi, W.N., Lee, J.S., Bui, T.V., Radu, R.A., Horwitz, J., and Travis, G.H. (2004). Rpe65 is a retinyl ester binding protein that presents insoluble substrate to the isomerase in retinal pigment epithelial cells. J. Biol. Chem. **279,** 635–643.

McClintock, B. (1984). The significance of responses of the genome to challenge. Science **226,** 792–801.

Morris, S.E., Turnbull, C.G., Murfet, I.C., and Beveridge, C.A. (2001). Mutational analysis of branching in pea. Evidence that *Rms1* and *Rms5* regulate the same novel signal. Plant Physiol. **126,** 1205–1213.

Napoli, C.A. (1996). Highly branched phenotype of the petunia *dad1–1* mutant is reversed by grafting. Plant Physiol. **111,** 27–37.

Napoli, C.A., Beveridge, C.A., and Snowden, K.C. (1999). Reevaluating concepts of apical dominance and the control of axillary bud outgrowth. Curr. Top. Dev. Biol. **44,** 127–169.

Napoli, C.A., and Ruehle, J. (1996). New mutations affecting meristem growth and potential in *Petunia hybrida* Vilm. J. Hered. **87,** 371–377.

Oh, S.A., Park, J.H., Lee, G.I., Paek, K.H., Park, S.K., and Nam, H.G. (1997). Identification of three genetic loci controlling leaf senescence in *Arabidopsis thaliana*. Plant J. **12,** 527–535.

Pfaffl, M.W. (2001). A new mathematical model for relative quantification in real-time RT-PCR. Nucleic Acids Res. **29,** e45.

Que, Q., Wang, H.-Y., English, J., and Jorgensen, R.A. (1997). The frequency and degree of cosuppression by sense chalcone synthase transgenes are dependent on transgene promoter strength and are reduced by premature nonsense codons in the transgene coding sequence. Plant Cell **9,** 1357–1368.

Ramakers, C., Ruijter, J.M., Lekanne Deprez, R.H., and Moorman, A.F.M. (2003). Assumption-free analysis of quantitative real-time polymerase chain reaction (PCR) data. Neurosci. Lett. **339,** 62–66.

Rameau, C., Bodelin, C., Cadier, D., Grandjean, O., Miard, F., and Murfet, I.C. (1997). New *ramosus* mutants at loci *Rms1*, *Rms3* and *Rms4* resulting from the mutation breeding program at Versailles. Pisum Genet. **29,** 7–12.

Rameau, C., Murfet, I.C., Laucou, V., Floyd, R.S., Morris, S.E., and Beveridge, C.A. (2002). Pea *rms6* mutants exhibit increased basal branching. Physiol. Plant. **115,** 458–467.

Redmond, T.M., Gentleman, S., Duncan, T., Yu, S., Wiggert, B., Gantt, E., and Cunningham, F.X. (2001). Identification, expression and substrate specificity of a mammalian beta-carotene 15,15'-dioxygenase. J. Biol. Chem. **276,** 6560–6565.

Redmond, T.M., Yu, S., Lee, E., Bok, D., Hamasaki, D., Chen, N., Goletz, P., Ma, J.X., Crouch, R.K., and Pfeifer, K. (1998). *Rpe65* is necessary for production of 11-*cis*-vitamin A in the retinal visual cycle. Nat. Genet. **20,** 344–351.

Richins, R.D., Scholthof, H.B., and Shepherd, R.J. (1987). Sequence of figwort mosaic virus DNA (caulimovirus group). Nucleic Acids Res. **15,** 8451–8466.

Schwartz, S.H., Tan, B.C., Gage, D.A., Zeevaart, J.A.D., and McCarty, D.R. (1997). Specific oxidative cleavage of carotenoids by VP14 of maize. Science **276,** 1872–1874.

Schwartz, S.H., Qin, X., and Loewen, M. (2004). The biochemical characterization of two carotenoid cleavage enzymes from Arabidopsis indicates that a carotenoid-derived compound inhibits lateral branching. J. Biol. Chem. **279,** 46940–46945.

Schwartz, S.H., Qin, X., and Zeevaart, J.A.D. (2001). Characterization of a novel carotenoid cleavage dioxygenase from plants. J. Biol. Chem. **276,** 25208–25211.

Simkin, A.J., Schwartz, S.H., Auldridge, M., Taylor, M.G., and Klee, H.J. (2004a). The tomato carotenoid cleavage dioxygenase 1 genes contribute to the formation of the flavor volatiles β-ionone, pseudoionone, and geranylacetone. Plant J. **40,** 882–892.

Simkin, A.J., Underwood, B.A., Auldridge, M., Loucas, H.M., Shibuya, K., Schmelz, E., Clark, D.G., and Klee, H.J. (2004b). Circadian regulation of the PhCCD1 carotenoid cleavage dioxygenase controls emissions of β-ionone, a fragrance volatile of petunia flowers. Plant Physiol. **136,** 3504–3514.

Smart, C. (1994). Gene expression during leaf senescence. New Phytol. **126,** 419–448.

Snowden, K.C., and Napoli, C.A. (1998). *Psl*: A novel *Spm*-like transposable element from *Petunia hybrida*. Plant J. **14,** 43–54.

Snowden, K.C., and Napoli, C.A. (2003). A quantitative study of lateral branching in petunia. Funct. Plant Biol. **30,** 987–994.

Sorefan, K., Booker, J., Haurogné, K., Goussot, M., Bainbridge, K., Foo, E., Chatfield, S., Ward, S., Beveridge, C., Rameau, C., and Leyser, O. (2003). *MAX4* and *RMS1* are orthologous dioxygenase-like genes that regulate shoot branching in Arabidopsis and pea. Genes Dev. **17,** 1469–1474.

Steeves, T.A., and Sussex, I.M. (1989). Patterns in Plant Development. (Cambridge, UK: Cambridge University Press).

Stirnberg, P., van de Sande, K., and Leyser, H.M.O. (2002). *MAX1* and *MAX2* control shoot lateral branching in *Arabidopsis*. Development **129,** 1131–1141.

Sussex, I.M., and Kerk, N.M. (2001). The evolution of plant architecture. Curr. Opin. Plant Biol. **4,** 33–37.

Tan, B.C., Schwartz, S.H., Zeevaart, J.A., and McCarty, D.R. (1997). Genetic control of abscisic acid biosynthesis in maize. Proc. Natl. Acad. Sci. USA **94,** 12235–12240.

Thompson, J.D., Gibson, T.J., Plewniak, F., Jeanmougin, F., and Higgins, D.G. (1997). The ClustalX windows interface: Flexible strategies for multiple sequence alignment aided by quality analysis tools. Nucleic Acids Res. **24,** 4876–4882.

Turnbull, C.G.N., Booker, J.P., and Leyser, H.M.O. (2002). Micrografting techniques for testing long distance-signalling in Arabidopsis. Plant J. **32,** 255–262.

Vandesompele, J., De Preter, K., Pattyn, F., Poppe, B., Van Roy, N., De Paepe, A., and Speleman, F. (2002). Accurate normalization of real-time quantitative RT-PCR data by geometric averaging of multiple internal control genes. Genome Biol. **3,** RESEARCH0034.

von Lintig, J., and Vogt, K. (2000). Filling the gap in vitamin A research. J. Biol. Chem. **275,** 11915–11920.

von Lintig, J., Dreher, A., Kiefer, C., Wernet, M.F., and Vogt, K. (2001). Analysis of the blind *Drosophila* mutant *ninaB* identifies the gene encoding the key enzyme for vitamin A formation *in vivo*. Proc. Natl. Acad. Sci. USA **98,** 1130–1135.

Woo, H.R., Chung, K.M., Park, J.H., Oh, S.A., Ahn, T., Hong, S.H., Jang, S.K., and Nam, H.G. (2001). ORE9, an F-box protein that regulates leaf senescence in Arabidopsis. Plant Cell **13,** 1779–1790.